Microstructure and mechanical properties of TiN dispersed Si_3N_4 ceramics via in-situ nitridation of coarse metallic Ti

Sotaro BABA ▪ The Institute of Scientific and Industrial Research (ISIR), Osaka University ▪ babasou23@sanken.osaka-u.ac.jp
Tomoyo GOTO ▪ The Institute of Scientific and Industrial Research (ISIR), Osaka University ▪ goto@sanken.osaka-u.ac.jp
Sunghun CHO ▪ The Institute of Scientific and Industrial Research (ISIR), Osaka University ▪ shcho@sanken.osaka-u.ac.jp
Tohru SEKINO ▪ The Institute of Scientific and Industrial Research (ISIR), Osaka University ▪ sekino@sanken.osaka-u.ac.jp

Érkezett: 2018. 07. 15. ▪ Received: 15. 07. 2018. ▪ https://doi.org/10.14382/epitoanyag-jsbcm.2018.34

Abstract
Titanium nitride (TiN) was formed by in-situ reaction of coarse metallic titanium (Ti) and silicon nitride (Si_3N_4) powder mixtures through hot-press sintering. Mechanical properties of the prepared Si_3N_4/TiN composite were observed. The Si_3N_4 raw powder containing Al_2O_3 and Y_2O_3 as sintering additives and large metallic Ti powders were mixed by the ball mill and then hot-pressed under a pressure of 30 MPa at 1500 °C for 0.5 h with different heating rate. The obtained sintered body had a unique structure in which polycrystalline and porous large TiN grains were dispersed in a dense Si_3N_4 matrix. The sintered composites were densified over 95 %, however, they contained around 26-38% of β-phase of Si_3N_4, which value was lower than that of monolithic Si_3N_4 sintered under the same condition. Although the hardness and the Young's modulus of the composite slightly decreased from the monolithic Si_3N_4, the fracture toughness was improved due mainly to the dispersion of large-sized TiN grains. It was considered that the matrix and the additive elements, which penetrated and formed oxide phases inside as well as at the grain boundaries of porous TiN grains through the sintering, improved the bonding between the TiN particles and the matrix to suppress the decrease of the mechanical properties.
Keywords: silicon nitride, nitridation reaction, sintering, TiN, microstructure formation, mechanical properties
Kulcsszavak: szilíciumnitrid, nitridálási reakció, szinterelés, TiN, mikrostruktúra kialakulása, mechanikai jellemzők

Sotaro BABA
Graduated master course in Nagaoka University of Technology, Japan (2015) and obtained PhD in September 2018 from Osaka University under supervision of Prof. T. Sekino at the Institute of Scientific and Industrial Research (ISIR). He is Assistant Professor in Mie University since November 2018.

Tomoyo GOTO
Graduated in Nagoya University, Japan and has PhD since 2012. She is appointed in Kyushu University and National Institute of Advanced Industrial Science and Technology (AIST), and at present she is an Assistant Professor in Prof. Sekino's Laboratory of ISIR, Osaka University.

Sunghun CHO
Graduated in Sunmoon University, Korea and has PhD since 2015, and continues his research as a post-doctoral scholar there. He is Assistant Professor in Prof. Sekino's Laboratory of ISIR, Osaka University since 2015.

Tohru SEKINO
Professor of the Department of Advanced Hard Materials, the Institute of Scientific and Industrial Research (ISIR), Osaka University since 2014. He has over 300 peer-reviewed scientific publications and more than 30 patents. He was awarded with various prizes including the Prizes for Science and Technology by the Minister of Education, Culture, Sports, Science and Technology (MEXT) Japan (2016), and the Ceramic Society of Japan Awards for Academic Achievements (2016).

1. Introduction

Silicon nitride ceramics (Si_3N_4) has high strength, high toughness, low density, excellent high temperature strength, low dielectric constant and is the most important material for structural materials. In order to expand the range of further utilization of silicon nitride material, improvement of fracture toughness value lower than general metal material which is one of factors of lowering reliability is required. Si_3N_4/metal composites consisted of metal dispersions having excellent elasticity and Si_3N_4 matrix have been developed for improving the brittleness of ceramics. Among various metals, Titanium (Ti) is lightweight and has a relatively high melting point, and is used as a base for heat resistant alloys, shape memory alloys and so on.

By using these two kinds of materials, Si_3N_4 and Ti in combination, it might be used as structural material that is lightweight and excellent in heat resistance and oxidation resistance. In fact, as the combination of Si_3N_4 and Ti metal, an active metal joining method using a Ti-added brazing filler was reported [1]. However, there was a problem to generate stress concentration at the joint interface and resultant residual stress that degraded bonding two phases.

A functionally-graded material (FGM), in which composition of two phases was gradually changed, was developed as a new method to improve mechanical reliability and to maintain their properties possessed by both materials. This has been studied as a way to further development of heterogeneous composite materials as well as solving the problem of stress concentration and residual stress at the joint interface of dissimilar materials. For example, *Shinohara* et al [2] developed a coating having thermal stress relaxation function by gradually-changed composition of partially-stabilized zirconia (PSZ) ceramic and NiCrAlY alloy to suppress thermal barrier coating degradation due to thermal stress at the interface between super alloy and ceramic thermal barrier coating under high temperature. In addition, *Tsuda* et al [3] fabricated a functionally graded material in which a graded layer of Ti-based ceramics was formed on the surface of a cemented carbide and introduced a gradient of thermal expansion coefficient into the material. As a result, they reported improvement of abrasion resistance and defect resistance as a cutting tool material.

However, when considering the combination of Ti with Si_3N_4, Ti easily reacts with Si_3N_4 and/or N_2 gas atmosphere during sintering to transform into titanium nitride (TiN),

so that partial Si_3N_4/TiN composite material is formed [4]. Studies on Si_3N_4/TiN composites have been reported so far, but most of them are focusing on improving electrical conductivity for addition of electrical discharge machinability to Si_3N_4. *Ahmadet* et al [5] fabricated the sintered composites by spark plasma sintering (SPS) of raw powder mixtures of Si_3N_4, sintering aid (oxides) and Ti powder, and analyzed the crystallography and conductivity. As a result, they obtained Si_3N_4 composite with sufficiently high conductivity that applicable to the electrical discharge machining. *Huang* et al [6] also produced a hot press sintered Si_3N_4/TiN composites using the in-situ nitridation reaction of Ti added to the raw powders, and reported the enhancement of bending strength of monolithic Si_3N_4 (around 400 MPa) to around 600 MP by the addition of 10 wt% Ti. *Lian* et al [7] reported a hot press sintering of Si_3N_4 and TiO_2 nanopowder mixtures in a nitrogen atmosphere. As a result, Si_3N_4/TiN nanocomposites with improved bending strength (1154 MPa) and fracture toughness and high electrical conductivity were achieved. Further, *Tatami* et al [8] reported the improvement of abrasion resistance for Si_3N_4/TiN nanocomposite fabricated from Si_3N_4, sintering aids and TiO_2 mixtures.

On the other hand, since Ti has high reactivity with Si_3N_4 and N_2 during sintering, Si_3N_4/Ti composite or FGM system might contain some weak interfacial reaction phase such as TiN and/or TiN-based compounds, which often hide fundamental Ti properties. In fact, not only materials physical properties but also consideration from the thermodynamic viewpoint concerning the reaction between Si_3N_4, Ti, TiN and TiO_2 have been discussed in these previous studies.

As pointed out here, Si_3N_4/TiN composite is expected to be utilized as a high strength material. For the development of these advanced composites consisted of Si_3N_4 ceramic and Ti metal, it is necessary to know the reaction behavior of Ti metal in silicon nitride in detail. The knowledge concerning the behavior of morphological change of TiN particles transformed from Ti in the sintered body produced by in-situ reaction of Ti with Si_3N_4 and N_2 gas, and the effect of the dispersed particles on the physical properties of the TiN composite can be expected to contribute to microstructures and physical properties control of Si_3N_4/TiN composite materials.

In this study, the effect of the morphology and transformation behavior of Ti particles to TiN grains in the hot press sintered body by changing the heating rate for the Si_3N_4 and Ti powder mixtures, which aimed to vary the total heating time during the sintering. Coarse Ti powder was used in this research to clarify the reaction behaviors and also to increase fracture toughness. The effect of these processing parameters on the phase and microstructure development, physical and mechanical properties of the sintered body was investigated and discussed.

2. Experimental procedure

2.1. Powder preparation and sintering

As a base composition of monolithic Si_3N_4 ceramic sample, α-Si_3N_4 powder (SN-E10, Ube Ind., Tokyo, Japan) was mixed with 2 wt% Al_2O_3 powder (AKP-30, Sumitomo Chem. Co. Ltd., Tokyo, Japan) and 5 wt% Y_2O_3 powder (Ishizu Co., Osaka, Japan) as sintering additives. As a composite sample, 10 wt% of Ti powder (TS-450, Toho Titanium Co. Ltd., Kanagawa, Japan) having a particle size of 45 μm or less was added to the monolithic composition. Each powders were placed in a resin bottle together with Si_3N_4 balls having diameter of 3 mm and ethanol as a mixing solution, and mixed by a wet ball mill for 24 h. The obtained slurry was dried using a vacuum evaporator. Then, the dried powder was aggregated by dry ball mill. After that, the mixed powders were passed through a sieve using a 500 μm sieve.

Then, 20 g of each raw powder mixture was put into graphite die with (44 mm of diameter) and hot press sintered at 1650°C for 0.5 h under 30 MPa of uniaxial pressure in N_2 gas atmosphere. The heating rate were changed in this experiments at 25, 30 and 40 °C·min^{-1}. The sintered samples were cut by diamond disc, grinded by #100 diamond grinding stone and polished by 9 to 0.5 μm of diamond slurry to obtain mirror surface. Hereafter, materials ID is denoted as SN_xx or SNTi_xx, where the SN and SNTi corresponds to the monolithic and 10wt% Ti added Si_3N_4 samples, and xx corresponds to the heating rate, 20, 30 and 40 °C·min^{-1}, respectively.

2.2. Material evaluations

The crystallographic phase of raw powders and sintered bodies were determined by X-ray diffraction method (XRD, D8 Advance, Bruker AXS GmbH, Karlsruhe, Germany). The β-type Si_3N_4 phase ratio (here as β) in the samples was calculated from XRD peak intensity of each phases of α-Si_3N_4 (ICDD PDF 010716479) and β-Si_3N_4 (ICDD PDF 000331160) using equation 1, where the α and β are the intensity (i.e. α + β = 1.0), $\alpha_{(hlk)}$ and $\beta_{(hlk)}$ are the intensity of each peaks of the α- and β-Si_3N_4, respectively.

$$\frac{\beta}{\alpha+\beta} = \frac{\beta(101)+\beta(210)}{\alpha(210)+\alpha(201)+\beta(101)+\beta(210)} \quad (1)$$

The density of samples were measured by Archimedes' method using samples immersed in toluene for 24 h. The microstructure were observed by using ultra high-resolution field emission scanning electron microscope (FE-SEM, SU-9000, Hitachi High-Technologies Co., Tokyo, Japan), and elemental analysis were carried out by energy dispersive X-ray spectrometer (EDX, X–Max100TLE, HORIBA Ltd., Kyoto, Japan) coupled in FE-SEM.

The Vickers hardness (*Hv*) was measured using a Vickers Hardness Tester (FV-310e, Future-tech Corp., Tokyo, Japan) on the polished surface with an indentation load of 98 N and holding time of 15 s. Further, the fracture toughness (K_{IC}) were evaluated by the indentation fracture (IF) method [9] using the Eq. (2) with the same condition as that of *Hv* measurement.

$$K_{IC} = 0.203\left(\frac{c}{a}\right)^{-\frac{3}{2}} a^{\frac{1}{2}} Hv \quad (2)$$

where, *c* and *a* are the length of median crack and half of diagonal of indentation.

The Young's modulus (*E*) were determined by the ultrasonic pulse echo method using a digital storage oscilloscope (DSOX3052T, Keysight, Tokyo, Japan) and an ultrasonic

pulser/receiver (Model 5072, PANAMETRICS, MA, USA). The Young's modulus value was calculated by Eq. (3) [10].

$$E = V_S^2 \rho \frac{3V_L^2 - 4V_S^2}{V_L^2 - V_S^2} \quad (3)$$

where, ρ is bulk density of sample, and V_L and V_S are sound velocity of measured longitudinal and transverse waves.

3. Results

3.1 Phase development and sinterability

Under the present experimental condition, well-sintered samples were obtained by hot press sintering at 1650°C for 0.5 h at a heating rate from 25 to 40 °C·min^{-1} in a N_2 gas flow. On the other hand, sufficiently densified sintered bodies were not obtained when the hot press was carried out under an Ar or vacuum conditions. Therefore, the samples sintered under the N_2 atmosphere have been further investigated hereafter.

Fig. 1 shows the XRD patterns of sintered bodies and raw powders. In a raw mixed powder, α-type of Si_3N_4 (ICDD PDF: 010716479) was only identified with sintering additives and metallic α-type of Ti (ICDD PDF: 010773482). On the other hand, the both α- and β-type of Si_3N_4 (ICDD PDF: 000331160) peaks were identified from the whole samples after sintering. In addition, TiN (ICDD PDF: 030650565) was identified from the composite samples (SNTi) instead of metallic Ti. It is generally known for the silicon nitride ceramic that the α-Si_3N_4 of raw powder transformed to β-Si_3N_4 during singeing by following dissolution and re-precipitation mechanism [11]. In the case of Ti added sintered body, the α-Ti peak was disappeared and nitrided metal phase as TiN appeared under the whole sintering, i.e. under the heating rate condition. Also, the titanium silicide phase that was often reported [5] was not identified in the present investigation.

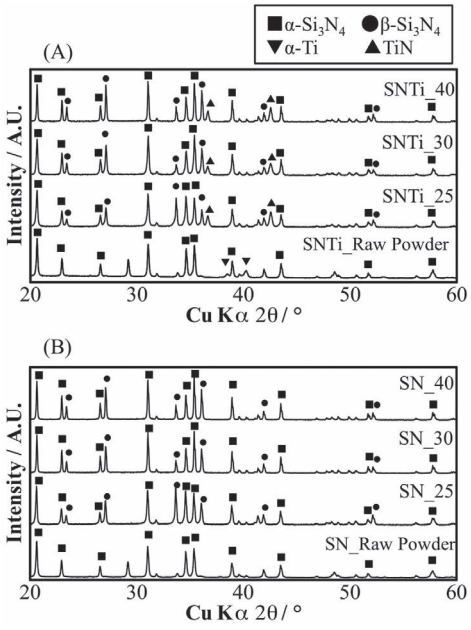

Fig. 1 XRD patterns of sintered bodies and raw powders for (a) monolithic (SN) and (b) Ti-added Si_3N_4 (SNTi) ceramics

1. ábra Szinterelt és nyers porok röntgendiffraktogramjai (a) monolitikus (SN) és (b) Ti adalékolt Si_3N_4 (SNTi) kerámiák

As mentioned above, in this study, an α/β mixed phase was obtained by the hot press sintering. Therefore, the β-ratio, which is the fraction of β-phase in the sintered Si_3N_4, was calculated from the XRD results using the Eq. (1). And the relationships between the β-ration and the heating rate of sintering was shown in *Fig. 2* together with that between the relative density and the heating rate. In the case of monolithic Si_3N_4, the β-ratio was 30-50% depend on the heating rate while the density was 3.236, 3.230 and 3.201 g·cm^{-3} at a heating rate of 25, 30 and 40 °C·min^{-1}, respectively. On the other hand, the β-ratio for the Ti-added samples was around 26 to 38 %, which values were slightly lower than that of monolithic Si_3N_4.

In contrast, the density values (3.321, 3.281 and 3.331 g·cm^{-3} at 25, 30 and 40 °C·min^{-1}, respectively) was slightly higher than the monolithic samples. In spite of the complex reaction of Ti phases among the sintered bodies, the theoretical density of Ti added sample was calculated by assuming 12.6 wt% of TiN dispersion in Si_3N_4 ceramic, which value was calculated by the nitridation of 10 wt% of Ti into TiN, resulted in the value of 3.362 g·cm^{-3} as the theoretical density of the samples. The relative densities were then obtained and reached to 95 TD% or more under all the sintering conditions (*Fig. 2.b*), indicating that a sufficiently densified sample was obtained. In the case of monolithic Si_3N_4, the relative density tended to decrease with increase in heating rate as shown in *Fig. 2.b*, however, both β-ratio and relative density of Ti dispersed sample showed lower values for the sample obtained from 30 °C·min^{-1}.

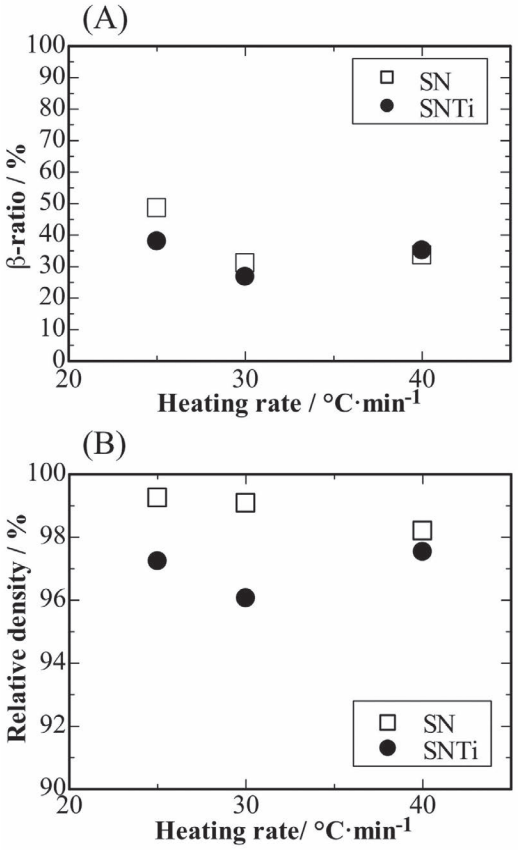

Fig. 2 Effects of heating rate on (a) β-ratio and (b) relative density for sintered samples

2. ábra Felfűtési sebesség hatása (a) a β-arányra és (b) a realtív sűrűségre a szinterelt mintákban

3.2 Microstructure

Fig. 3 shows a SEM image of Ti particle in the raw mixture powder. The average diameter of Ti particles in the raw mixture powder were 5.83 μm which was smaller than the raw Ti particles (<45 μm) by ball milling. It was also observed that raw Si_3N_4 and additives powders, which primary size was much smaller than that of Ti, were adhered around large Ti particle.

Fig. 4 shows the optical image on the polished surface of the sintered body. The surface of monolithic Si_3N_4 was smooth, and a few pores were observed (*Fig. 4.a*). On the other hand, large particles of several tens of micrometers were found to disperse in the matrix of the Ti-added composite sample (*Fig. 4.b)*. The color of these large particles were gold, which was the typical color of the TiN compound, and is consisted with the result of XRD analysis.

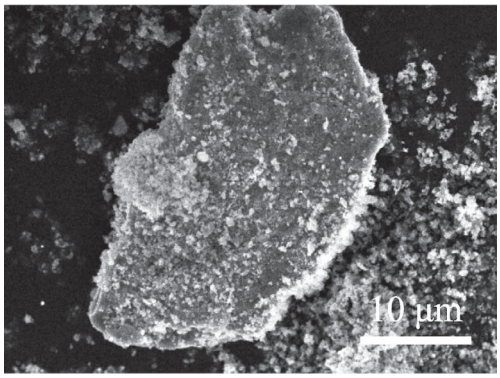

Fig. 3 SEM image of titanium particle in the raw mixture powder. Fine particles are Si_3N_4 raw material
3. ábra Titán részecskék elektronmikroszkópos képe a nyers por keverékben. A finom részecskék a nyers Si_3N_4 anyag

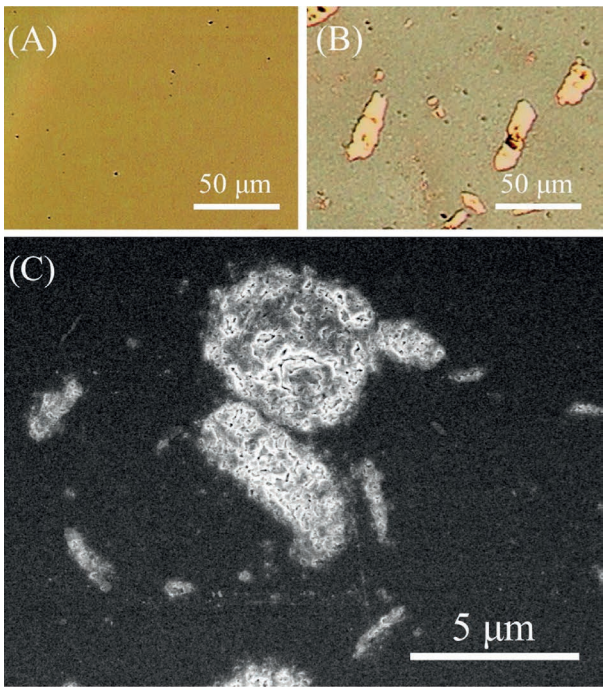

Fig. 4 Optical images on the polished surface of the sintered bodies for (a) monolithic Si_3N_4 (SN_25) and (b) Ti-added Si_3N_4 (SNTi_25), and SEM image on the surface for (c) Ti-added Si_3N_4 (SNTi_40)
4. ábra Szinterelt minták polírozott felületének optikai képe (a) monolitikus Si_3N_4 (SN_25) és (b) Ti adalékolt Si_3N_4 (SNTi_25), és elektronmikroszkópos felvétel a felületen (c) Ti adalékolt Si_3N_4 (SNTi_40) anyagra vonatkozóan

To evaluate structures of dispersed phase in more detail, SEM observation and EDS analysis for the formed TiN particles were carried out, and the results are shown in *Fig. 5*. The Ti particle used as raw powder had a dense structure, however, porous structure and inner grain boundaries were observed in Ti-derived particles. Ti and N was detected from the corresponding Ti-derived particles by EDS. Nitrogen was found also in the center of the particle, indicating that N penetrated to the central part of Ti particles. From the matrix region, Si, Al and Y as well as N derived from Si_3N_4 and additives were detected. Based on the above results as well as the XRD (*Fig. 1*), it was clear that the metal Ti particles used as a raw material was nitrided during sintering to form TiN, thus obtained material by this sintering method was Si_3N_4/TiN composite.

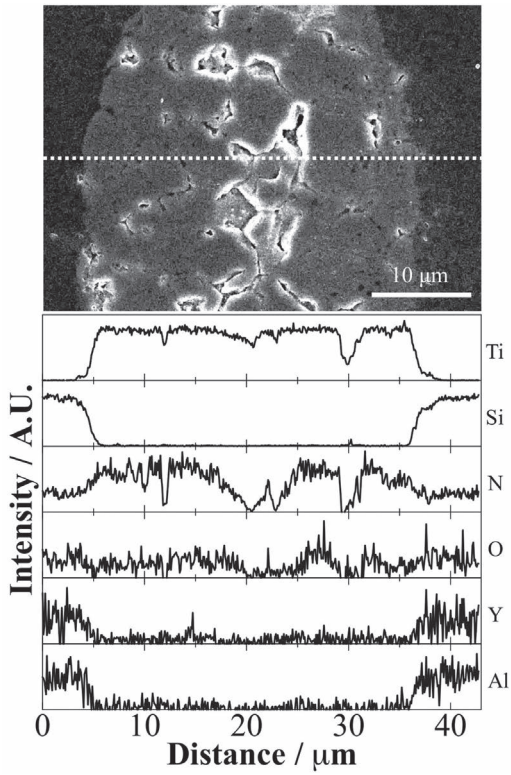

Fig. 5 SEM image of titanium-derived coarse TiN particle and EDS line analysis results (scan on broken-line) for the cross-sectional surface of the SNTi_25 sample, where the EDS line scan was taken for the parallel to the uniaxial pressing direction
5. ábra Elektronmikroszkópos felvétel Ti generált TiN szemcséről és EDS vonal elemzés (felvétel törött felületen) a SNTi_25 minta keresztmetszeti felületén, ahol az EDS vonal elemzés iránya párhuzamos az egytengelyű nyomás irányával

Fig. 6 shows the relationships between heating rate and equivalent diameter of dispersed TiN particle in the sintered bodies, where the diameter was calculated by the image analysis method from obtained SEM images. The diameter value of the dispersed phase was 12.29, 10.25 and 9.98 μm at the heating rate of 25, 30 and 40 $^{o}C{\cdot}min^{-1}$, respectively, and tended to decrease as the heating rate increased. The diameter of the dispersed particle was approximately two times larger than that of used Ti raw powder, which was 5.8 μm, showing the particle size increase was governed after the hot press sintering.

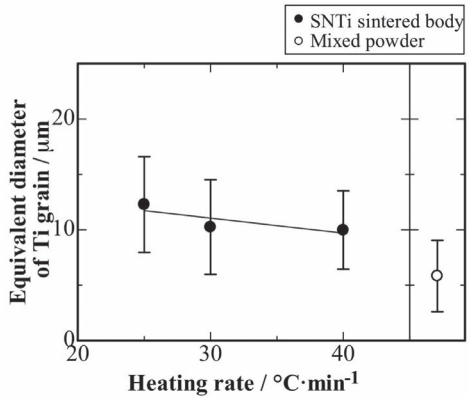

Fig. 6 The relationship between heating rate and equivalent diameter of TiN particles formed in the Si_3N_4 sintered samples
6. ábra A felfűtési sebesség és a kialakuló TiN szemcsék egyenértékű átmérőjének összefüggése szinterelt Si_3N_4 mintákban

4. Discussion

Generally, sintered Si_3N_4 is well known to be formed by a dissolution of α phase in liquid phase by sintering additives and followed re-precipitation and growth as to be β phase grains [11]. In the present study, the mixed phase of α- and β-Si_3N_4 was observed a mentioned before (*Fig. 1*). In this study, we selected a sintering condition with a relatively higher heating rate (> 25 °C·min^{-1}), lower sintering temperature (1650°C) and shorter holding time (~ 0.5 h) compared to the commonly used condition of Si_3N_4 sintering, above 1800°C [11]. For this reason, unlike the commonly obtained sintered body with single β-phase, the present samples contained the both β- and α-phases. Nevertheless, sintered samples were fairly densified, more than 95% of relative density (see *Fig. 2*). This phenomenon was often reported for the Si_3N_4 sintered by pulse electric current sintering (PECS, also described as SPS) which enables rapid and short-time sintering [5, 12].

4.1 Effect of Ti addition to Si_3N_4 on physical properties

Fig. 7 shows the relationship between the heating rate and the Young's modulus. In the Si_3N_4 monolith, the Young's modulus tended to decrease slightly with increase in heating rate. On the other hand, Young's modulus of Ti-added samples slightly increased with the heating rate. The theoretical Young's modulus of the Si_3N_4 composite containing 12.6 wt% of TiN (by considering complete transformation of Ti to TiN as mentioned before) was estimated by the Hill's equation [13], and the value was calculated to be 325 GPa. However, the observed Young's modulus of the present samples was lower than the calculated value, which was around 270 GPa (30 °C·min^{-1}) to 305 GPa (40 °C·min^{-1}).

As found by the SEM investigation, the present composites contained aggregated but porous polycrystalline TiN regions (see *Fig. 5*) which dispersed in dense Si_3N_4 matrix. It imply us that the porosity of the TiN particles might affect on the decrease in density of the sintered samples, and then resultantly on the decreased Young's modulus. Thus, at first, the density of TiN particle (d_{TiN}) dispersed in sintering body was calculated from the relationship between density and mass concentration by the Eq. (4).

$$d_{TiN} = \frac{W_{TiN} d_c d_m}{(1-W_{TiN})(d_m - d_c) + W_{TiN} d_m} \quad (4)$$

Where d_m and d_c is the measured density of monolithic Si_3N_4 and TiN dispersed Si_3N_4 composite, respectively, and W_{TiN} is the mass concentration of TiN in the sintered body (12.6 wt%). Further, the porosity in the TiN particle region (P_{TiN}) was taken into account and was calculated from the relationship between the density and the porosity by Eq. (5),

$$P_{TiN} = 1 - \frac{d_{TiN}}{d_{th,TiN}} \quad (5)$$

where, $d_{th,TiN}$ is the theoretical density of TiN (5.45 g·cm^{-3}).

Then, the Young's modulus of porous TiN grain (E) was calculated using the Eq. (6) [14] representing the porosity dependency of the elastic modulus of the porous body.

$$E = E_0(1 - P_{TiN}) \quad (6)$$

Were E_0 is the Young's modulus of fully-densified TiN (390 GPa). *Table 1* shows the calculated porosities of the TiN particle and Young's modulus. The porosity of TiN particle was estimated to 13, 32 and 24% at 25, 30 and 40 °C·min^{-1}, respectively. These values seems to be reasonable by considering porous morphology of TiN grains observed by SEM image in *Fig. 5*. On the other hand, the Young's modulus of the porous TiN particles was estimated to be about 294, 265 and 339 GPa at 25, 30 and 40 °C·min^{-1}, respectively. High porosity and low Young's modulus were observed for the sample sintered at 30 °C·min^{-1}, which was due to the low density for the sample.

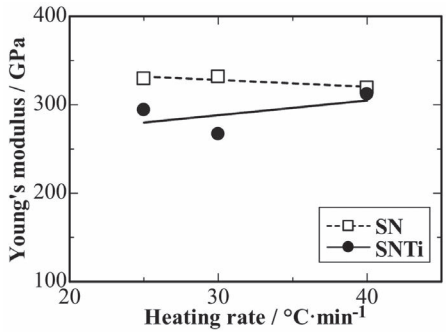

Fig. 7 Effect of heating rate on the Young's modulus for sintered Si_3N_4 samples
7. ábra A felfűtési sebesség és a rugalmassági modulus összefüggése szinterelt Si_3N_4 mintákban

Heating rate / °C·min-1	*PTiN* / %	*E* / GPa
25	24	294
30	32	265
40	13	339

Table 1 Calculated porosity and Young's modulus of TiN particle within the sintered Si_3N_4 samples. The values were estimated from each density data
1. táblázat Számított porozitás és rugalmassági modulus a TiN szemcsében a szinterelt Si_3N_4 mintákban. Az értékek becsült mennyiségek az egyes sűrűség adatok alapján

4.2 Effects of large and porous TiN grain on the mechanical properties.

Fig. 8.a shows the relationship between heating rate and the Vickers hardness. The hardness of the Si_3N_4 monolithic

was about 18 GPa, and the effect of the heating rate was not confirmed. The hardness of TiN dispersed samples was around 15 GPa, which was slightly lower than Si_3N_4 monolith. However, as discussed above, the *Hv* of composites was reasonable by considering the fact that large but porous TiN particles were dispersed in.

Fig. 8.b shows the relationship between heating rate and fracture toughness measured by the indentation fracture method. The fracture toughness of the monolithic Si_3N_4 showed a tendency to slightly decrease with increase in heating rate. On the other hand, the TiN dispersed samples showed an opposite tendency, and the value increased to 5.8 MPa·m$^{1/2}$ at 40 °C·min^{-1} which was higher than the toughness value of the monolithic Si_3N_4 sintered at the same condition.

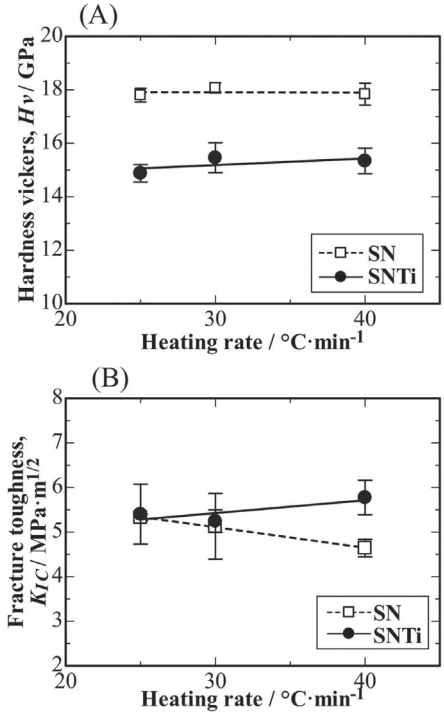

Fig. 8 Effect of heating rate on mechanical properties for sintered samples, (a) Hardness and (b) Fracture toughness
8. ábra A felfűtési sebesség hatása szinterelt minták mechanikai jellemzőire, (a) keménység és (b) törési szívósság

To discuss the mechanical properties of the present Si_3N_4/TiN composites from viewpoint of the crystalline phase of Si_3N_4 matrix, i.e. the effect of α/β phase, the relationships between these mechanical properties and β-ratio of Si_3N_4 matrix were shown in *Figure 9*. It is reported that the α-Si_3N_4 single crystal has 1.3 times higher hardness value that that of β-Si_3N_4 [15]. It is thus easily predicted that hardness declined as the β-ratio increases. In fact, *Kawaoka* et al [12] reported that the hardness and the Young's modulus decreased while the fracture toughness increased when the β-ratio increased for the spark plasma sintered Si_3N_4.

In the present study, however, the hardness of both monolithic and TiN dispersed Si_3N_4 did not depend strongly on the β-ratio (*Fig. 9.a*) although the value was higher for the monolithic Si_3N_4, which was, as discussed before, due to the dispersion of porous TiN phase. The reason of this behavior is regarded as the trade-off relation between the decreased hardness due to the density degradation and the increase in hardness due the increased α-Si_3N_4 ratio in the samples.

It is well-known that fracture toughness of sintered Si_3N_4 generally increases with grain growth of β-Si_3N_4 particles, especially formation of elongated large β-grains, resulting in high fracture toughness for high β conversion ratio [12]. In the present case, the toughness value seemed to be higher for the higher β-ratio. However, the correlation between the β-ratio and the fracture toughness was not distinct (*Fig. 9.b*).

For the TiN dispersed samples, it was considered that the fracture toughness value seemed to be affected more by the characteristics of the dispersed TiN; Sample SNTi_40 (40 °C·min^{-1}) showed the highest toughness and the lowest porosity in dispersed TiN (P_{TiN} = 13%, see *Table 1*), while the SNTi_30 (30 °C·min^{-1}) containing porous TiN (P_{TiN} = 32%) exhibited the lowest toughness among the composites. These fact imply us that the microstructural characteristic of dispersed TiN grains, i.e. porous structure, is more dominantly affect on the fracture toughness than the β-ratio of matrix.

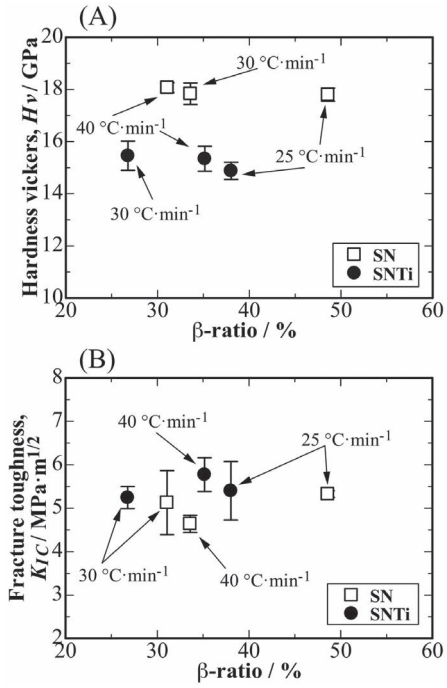

Fig. 9 The relationship between β-ratio and (a) Hardness, (b) Fracture toughness and (c) Young's modulus of sintered samples
9. ábra Összefüggések a β–aránnyal (a) keménység, (b) törési szívósság és (c) rugalmassági modulus a szinterelt mintákban

4.3 Microstructural characteristics of dispersed TiN particles

Although the Ti particle of the raw powder was large (*Fig. 3*), Ti-derived grains in the sintered body were polycrystalline but porous structure as explained before (*Fig. 4.c*). Thus it is said that the present Si_3N_4-based composite has a unique structure, where porous TiN grains were dispersed in Si_3N_4 matrix. The reason why such a complicated structure is formed will be discussed below. It should be considered that the Ti particles expanded during the reaction (transformation) to TiN. The mass increase rate when Ti (molecular weight: 47.96 g·mol^{-1}

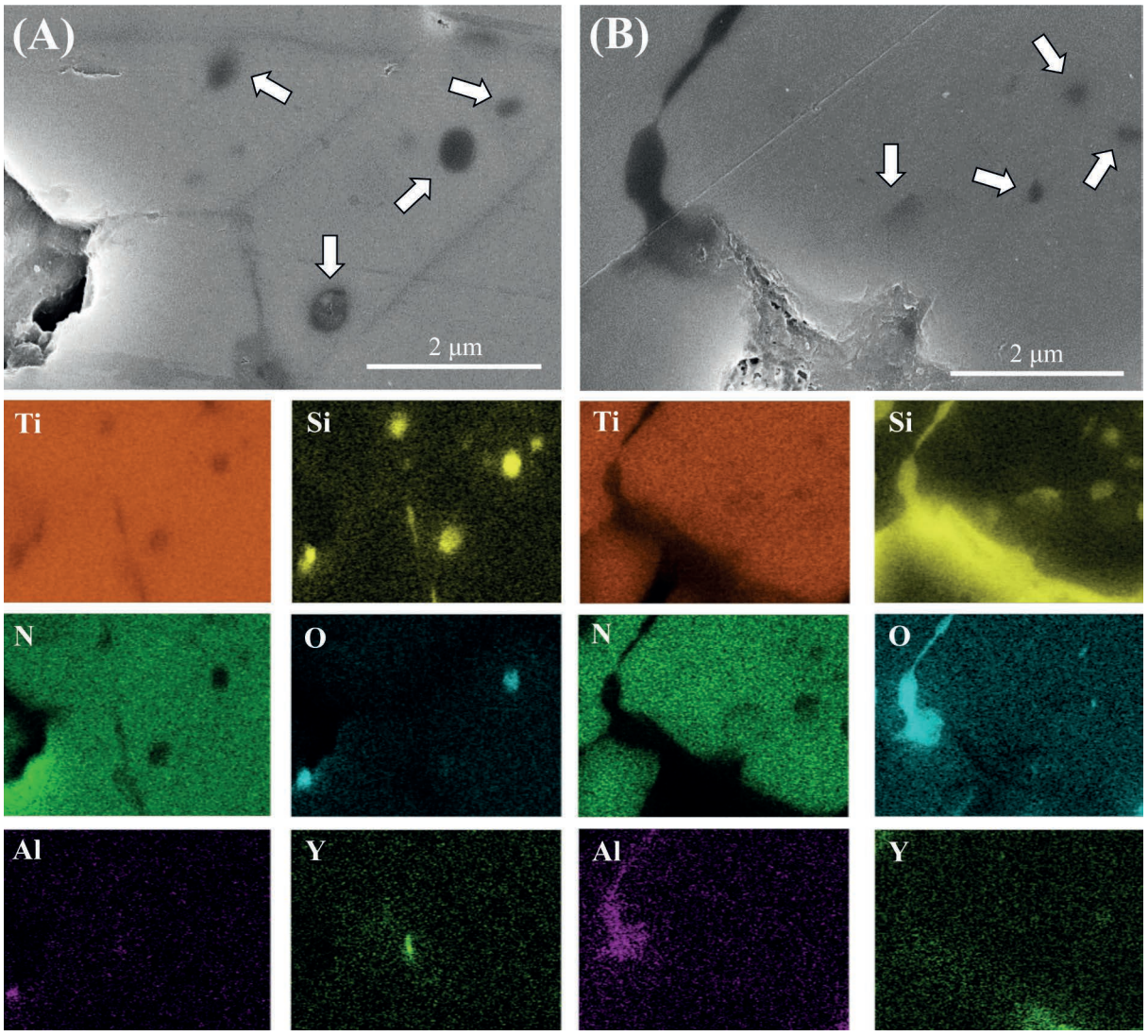

Fig. 10 Magnified SEM image of the center of TiN grain and corresponding elemental mapping images of Ti, Si, N, O, Al and Y for the samples (a) SNTi_25 and (b) SNTi_30
10. ábra Felnagyított elektronmikroszkópos felvétel a TiN szemcse középpontjában és a hozzá tartozó elemanalízis (Ti, Si, N, O, Al és Y) a mintákban (a) SNTi_25 és (b) SNTi_30

density: 4.51 g·cm^{-3}) transforms to TiN (weight: 61.96 g·mol^{-1}, density: 5.45 g·cm^{-3}) is 1.29, while the volume increase rate is calculated to be 1.068, which corresponds to only 2.2 % (1.022 times) increase in equivalent particles diameter. However, in this study, average grain size of dispersed TiN in the sintered Si_3N_4 (SNTi_25; 25 °C·min^{-1}) was 2.1 times larger than that of used raw Ti particles (see *Fig. 6)*. Therefore, it is not able to explain the reason of larger TiN by the chemical reaction (nitridation of Ti), and it is considered to be a minor role.

Magnified SEM and elemental mapping images of inside of TiN grains in the sintered body for SNTi_25 (heating rate of 25 °C·min^{-1}) and SNTi_30 (30 °C·min^{-1}) are shown in *Figs. 10.a* and *10.b*, respectively. It was clearly seen that the Ti-derived grain was polycrystalline structure with grain boundaries. In addition, some finer particulates which size is around 1 µm or less can be seen within the grains (see arrows in SEM images of *Fig. 10*). From element mapping results, Ti and N was uniformly detected from the whole area except pores, grainboundary and finer particles mentioned above, which results well agree to the fact previously discussed that the Ti was converted to the TiN during sintering. On the other hand, Si was found in the finer particles inside of the TiN and at some part of grain boundaries of TiN. Oxygen was also detected from not all but some region of Si detected (particulates and grainboundary). In addition, Al was often detected from the grain boundary phase together with Si and O (see *Figs. 10.a* and *10.*b). These results implied that the particulates inside of TiN was SiO_2 and Si, which might be formed or precipitated by the complicated reaction during sintering. At the grainboundary of formed TiN, SiO_2 or Al-Si-O compound were also precipitated during the reaction.

From these facts, it was considered that Si, Al, Y and O elements in Si_3N_4 and additives (Al_2O_3 and Y_2O_3) might diffused into the Ti particles during the nitridation reaction or into the formed TiN phase at the late stage of sintering. In the TiN regions, some oxides consisted of SiO_2 or Al-Si-O were found as mentioned above. These silica-based oxides were known to have lower melting temperature and to form glassy phase, and thus liquid phase of these oxides might exist during sintering that promoted reaction of TiN with Al and/or O and formation of Al-Si-O phases at the boundaries among TiN regions. Based on these results, the formation of coarse and porous TiN grains within Si_3N_4 matrix as well as enlargements of TiN grain size

more than primary Ti particles might be considered due to the combination of several factors as described follows.

Reaction and followed solid solution formation of constituent elements, especially Si-O and/or Si-Al-O based compounds near the Ti particles, should be taken place at first. In fact, grain boundary phases containing Si and O as major elements and Al, Y and Ti as minor elements. These grain boundary phases seemed to be generated form a liquid phase, and they were penetrated and precipitated into the internal grain boundary of polycrystalline TiN particles produced from Ti, thereby dividing primary Ti particles and increasing the equivalent diameter of Ti-based particles. The fine particulates within TiN, which were consisted mainly from Si-O or Si (*Fig. 10*), were considered to be formed by precipitation during sintering followed by the diffusion of corresponding elements in the raw materials into Ti particles.

Before or at the same time, nitridation of metallic Ti might be taken place by the direct reaction of Ti with N_2 atmosphere, or by the reaction with Si_3N_4 particles, because the reactivity of Ti with nitrogen is thermodynamically high. Reaction of nitrides with liquid phase might promote further diffusion of elements, such as Y etc. into the TiN, which could be seen in small amount but uniform distribution of Si, O and Y within the TiN particles existing as solid solution or precipitates as fine particles within TiN (see for example Si, O and Y in *Fig. 10.a*).

In addition, the effect of pressurization, i.e. mechanical uniaxial pressing during sintering should be considered. In this study, sintering was performed by hot press method at a high temperature of 1650°C, which corresponded to 0.99 T_m of Ti metal, extremely close to the melting point of Ti (T_m = 1668°C). At this temperature, Ti was sufficiently softened, and hence it might easily react with other components including Si_3N_4, nitrogen and formed oxide glassy phases.

In the case of nano-sized TiN dispersed dense Si_3N_4 composites, it was reported that the addition of several tens of volume percents of TiN was necessary to achieve the enhanced toughness [6, 7]. In this study however, Si_3N_4 composites containing porous TiN grains, in which the porosity of around 20 vol%, exhibited decreased hardness while slightly increased fracture toughness compared to the monolithic Si_3N_4 sintered ceramic by addition of only 10 wt% of Ti powder to Si_3N_4 matrix.

It is suggested that the formation of grain boundary phases within the porous TiN regions might improve bonding between constituent TiN particles with the porous regions, i.e. strengthening porous TiN structures, and also contribute to make better bonding between porous TiN and Si_3N_4 matrix, implying us that the dispersing coarse Ti particles and promotion of reaction to form porous TiN grains would be advantageous to develop Si_3N_4-based composites with improved mechanical properties by using commercially-available coarse metal powders.

5. Conclusions

Coarse-grained Ti metal powder was added by 10 wt% to Si_3N_4 raw powder together with Al_2O_3 and Y_2O_3 sintering additives, and the mixtures were hot-press sintered in a nitrogen atmosphere under an uniaxial-pressure of 30 MPa at 1650°C for 0.5 h with different heating rate. Effect of heating rate for hot-press sintering was investigated for the obtained Si_3N_4-based composites. The TiN grains were finally dispersed in the Si_3N_4 sintered bodies due to the reaction of Ti with Si_3N_4 and/or N_2 atmosphere during sintering. The following conclusions were obtained through the structural and mechanical properties investigations.

Coarse Ti powders reacted to form TiN grains during sintering. It was found that the formed TiN grains consisted from polycrystalline and porous TiN having oxides grain boundary phases of Si, O, Al and some minor elements. These implied that the obtained Si_3N_4 sintered body was complicated composite structure consisted of porous TiN grains (porosity of 13 to 32%) dispersed in dense Si_3N_4 matrix.

The Si_3N_4 matrix had the mixed phase of α- and β-type Si_3N_4, where the β-phase of around 26 to 38%, due to the relatively lower sintering temperature and higher heating rate for sintering. However, matrix itself was mostly densified of over 95% under the present sintering conditions.

Polycrystalline and porous TiN grains were much larger (~2 times) than the used coarse Ti particles and as well as than the theoretically-estimated particle size of nitrided Ti. It was considered that the reaction between Ti and other compounds such as Si_3N_4, Al_2O_3 etc. and resultant formation of glassy phase within the TiN regions might contribute to the enlargement of particle size from Ti to porous TiN during sintering.

Comparing with Si_3N_4 monolithic samples, Ti-added samples exhibited lower hardness and Young's modulus due to the porous structure of dispersed TiN grains. However, fracture toughens slightly enhanced than that for monolithic Si_3N_4. The present composite contained the both α and β-Si_3N_4 that suspected the lower toughness due to the lesser amount of elongated β-grains of matrix, however, the increased toughness was considered due to the dispersion of porous but large TiN grains in the matrix.

6. Acknowledgements

This work was supported by the program Dynamic Alliance for Open Innovation Bridging Human, Environment and Materials in Network Joint Research Center for Materials and Devices (MEXT, Japan).

References

[1] Carim, A. H. (1990): Transitional Phases at Ceramic–Metal Interfaces: Orthorhombic, Cubic, and Hexagonal Ti-Si-Cu-N Compounds. *Journal of the American Ceramic Society*, Vol. 73, pp. 2764-2766. https://doi.org/10.1111/j.1151-2916.1990.tb06762.x

[2] Shinohara, Y. – Imai, Y. – Ikeno, S. – Shiota, I. – Fukushima, T. (1992): Thermal stability of NiCrAlY/PSZ by plasma twin torches method, *ISIJ International*, Vol. 32, pp. 893-901. https://doi.org/10.2355/isijinternational.32.893

[3] Tsuda, K. – Ikegaya, A. – Nomura, T. (2000): Development of functionally graded sintered hard material, *Journal of Powder Metallurgy*, Vol. 47, pp. 487-495. https://doi.org/10.1179/pom.1996.39.4.296

[4] Wriedt, H.A. – Murray, J. L. (1987): The N-Ti (Nitrogen-Titanium) System, *Bulletin of Alloy Phase Diagrams*, Vol. 8, pp. 378-388. https://doi.org/10.1007/BF02869274

[5] Ahmad, N. – Sueyoshi, H. (2010): Properties of Si_3N_4-TiN composites fabricated by spark plasma sintering y using a mixture of Si_3N_4 and Ti powders, *Ceramics International*, Vol. 36, pp. 491-496. https://doi.org/10.1016/j.ceramint.2009.09.029

[6] Qiliang, H. – Juan, C. – Wei, P. – Jian, C. – Jie, L. (1997): In situ processing of TiN/Si_3N_4 composite by Ti-Si_3N_4 solid state reaction, *Material Letters*, Vol. 31, pp. 221-225. https://doi.org/10.1016/S0167-577X(96)00277-7

[7] Gao, L. – Li, J. – Kusunose, T. – Niihara, K. (2004): Preparation and properties of TiN-Si_3N_4 composites, *Journal of the European Ceramic Society*, Vol. 24, pp. 381-386. https://doi.org/10.1016/S0955-2219(03)00218-8

[8] Tatami, J. – Watanabe, H. – Wakihara, T. – Yoneya, K. – Meguro, T. (2008): Development of Nano-particle Dispersed Si_3N_4 Ceramics Using Composite Powders Prepared by Mechanical Treatment, *Funsai* (in Japanese), Vol. 51, pp. 52-56.

[9] Nihara, K. (1983): A fracture mechanics analysis of indentation-induced Palmqvist crack in ceramics, *Journal of Materials Science Letters*, Vol. 2, No. 5, pp. 221-223. https://doi.org/10.1007/BF00725625

[10] Nishida, T. – Yasuda, E. (Ed.) (1986): Evaluation of mechanical properties of ceramics, *Nikkan Kogyo Shinbun Sya*, Tokyo Japan.

[11] Mitomo, M. – Mizuno, K. (1986): Sintering Behavior of Si_3N_4 with Y_2O_3 and Al_2O_3 Addition, *Yogyo Kyokaishi* (in Japanese), Vol. 94, No. 1085, pp. 106–111. https://doi.org/10.2109/jcersj1950.94.106

[12] Kawaoka, H. – Adachi, T. – Sekino, T. – Choa, Y. – Gao, L. – Niihara, K. (2001): Effect of α/β phase ratio on microstructure and mechanical properties of silicon nitride ceramics, *Journal of Materials Research*, Vol. 16, No. 8, pp. 2264-2270. https://doi.org/10.1557/JMR.2001.0311

[13] Miki, M. – Fukuda, T. – Motoki, S. – Hohjo, M. (1997): Composite Material, *Kyoritsu Shuppan*, Tokyo Japan, pp.70-72.

[14] Kondo, R. (1978): Porous material –Properties and Application, *Gihodo Shuppan*, Tokyo Japan, pp.174-181.

[15] Niihara, K. – Hirai, T. (1978): Hardness anisotropy of α-Si_3N_4 single crystal, *Journal of Materials Science*, Vol. 13, pp. 2276-2278. https://doi.org/10.1007/BF00541688

Ref.:
Baba, Sotaro – **Goto,** Tomoyo – **Cho,** Sunghun – **Sekino,** Tohru: *Microstructure and mechanical properties of TiN dispersed Si_3N_4 ceramics via in-situ nitridation of coarse metallic Ti*
Építőanyag – Journal of Silicate Based and Composite Materials, Vol. 70, No. 6 (2018), 195–203. p.
https://doi.org/10.14382/epitoanyag-jsbcm.2018.34

5th Euro
BioMAT
2019

European Symposium and Exhibition on Biomaterials and Related Areas

08. - 09. May 2019
Weimar, Germany

https://biomat2019.dgm.de

DGM

The Scope

Based on the huge success of the previous four **Euro BioMAT** Symposia 2011 in Jena and in 2013, 2015 and 2017 in Weimar this international conference will be held every two years in the Jena-Weimar region.

The symposium **Euro BioMAT 2019, 08.-09. May 2019,** addresses the growing interest of science and industry in the different aspects of the creation, characterization, testing and application of biomaterials and closely related areas. The motivation is not only the recent scientific progress and new challenges in this exciting, strongly interdisciplinary field of science and engineering. Materials scientists, physicists, chemists, biologists in industrial R&D as well as medical professionals are increasingly facing situations, where materials are confronted with high performance requirements and a challenging biological environment at the same time.

Much of the growth in the area of biomaterials emerged in the USA and Asia over the last years but Europe is gaining ground with a fast and steady growth in this field. The German Materials Society (DGM) and its panel of experts in biomaterials address these developments with the **Euro BioMAT 2019** in Weimar.
Euro BioMAT 2019 will present and discuss the current state of progress and novel trends in development, characterization, application, testing and modelling of biomaterials in basic science and industry. In addition, this symposium will bring together experts in closely related areas, such as biomimetics, biomineralization and biopolymers.

The organizers at the DGM feel a need to serve the European biomaterials community beyond other European and world biomaterials congresses with a compact two-day meeting which brings together fascinating science and stimulating people in a delightful setting in historic Weimar in the very heart of Europe. The program of the **Euro BioMAT 2019** will comprise several invited plenary lectures as well as oral and poster presentations. The organizers look forward to receiving many contributions to the **Euro BioMAT 2019**.

We look forward to seeing you in Weimar 2019!

Klaus D. Jandt, Chairman
Friedrich Schiller University Jena, Germany

Thomas F. Keller, Vice Chairman
DESY Hamburg, Germany